High-resolution Peripheral Quantitative Computed Tomography Imaging in the Assessment of Periarticular Bone of Metacarpophalangeal and Wrist Joints

Sujay Nagaraj, Stephanie Finzel, Kathryn S. Stok, Cheryl Barnabe, and the SPECTRA Collaboration

ABSTRACT. ***Objective.*** To synthesize descriptions of periarticular findings at the metacarpophalangeal (MCP) and wrist joints in different types of arthritis and in the normal state imaged by high-resolution peripheral quantitative computed tomography (HR-pQCT); to assemble the literature reporting on the ability of HR-pQCT to detect findings relative to other imaging modalities; and to collate results on the reproducibility of image interpretation.

Methods. A systematic literature review was performed using terms for HR-pQCT and MCP or wrist joints using medical literature databases and conference abstracts. Any study describing predefined pathology findings, comparison to another radiographic technique, or a measure of reproducibility was included with no limitation by disease state.

Results. We identified 44 studies meeting inclusion criteria from the 1901 articles identified by our search. All 44 reported on pathology findings, including erosions (n = 31), bone microarchitecture (n = 10) and bone mineral density (n = 10) variables, joint space evaluation (n = 7), or osteophyte characterization (n = 7). Seventeen of the studies compared HR-pQCT findings to either plain radiography (n = 9), ultrasound (n = 4), magnetic resonance imaging (n = 5), or microcomputed tomography (n = 2), with HR-pQCT having high sensitivity for erosion detection. Twenty-four studies included an assessment of reproducibility with good to excellent metrics, and highlighting the critical importance of positioning when assessing joint space variables.

Conclusion. Despite high sensitivity for erosion detection and good reproducibility, more research is required to determine where HR-pQCT can be applied to enhance our understanding of periarticular bone changes in a variety of arthritis conditions. (J Rheumatol 2016;43:1921–34; doi:10.3899/jrheum.160647)

Key Indexing Terms:
RADIOGRAPHIC MICROTOMOGRAPHY WRIST METACARPOPHALANGEAL JOINT ARTHRITIS DIAGNOSTIC IMAGING JOINTS

From the Faculty of Arts and Sciences, Queen's University, Kingston, Ontario, Canada; Department of Rheumatology and Clinical Immunology, University Medical Center Freiburg, Faculty of Medicine, University of Freiburg, Freiburg, Germany; Institute for Biomechanics, ETH Zurich, Zurich; Scanco Medical AG, Bruettisellen, Switzerland; Department of Medicine, and Department of Community Health Sciences, Cumming School of Medicine, University of Calgary, Calgary, Alberta, Canada.

S. Nagaraj was funded by an Alberta Innovates-Health Solutions Summer Studentship. C. Barnabe is a Canadian Institutes of Health Research New Investigator.

As part of a supplement series from SPECTRA on HR-pQCT, this report was reviewed internally and approved by the Guest Editors for integrity, accuracy, and consistency with scientific and ethical standards.

S. Nagaraj, Undergraduate Student, Faculty of Arts and Sciences, Queen's University; S. Finzel, MD, MBA, HCM, Department of Rheumatology and Clinical Immunology, University Medical Center Freiburg, Faculty of Medicine, University of Freiburg; K.S. Stok, PhD, Institute for Biomechanics, ETH Zurich and Scanco Medical AG; C. Barnabe, MD, MSc, Associate Professor, Department of Medicine and Department of Community Health Sciences, Cumming School of Medicine, University of Calgary; SPECTRA Collaboration Members are listed in Appendix 1.

Address correspondence to Dr. C. Barnabe, 3330 Hospital Drive NW, Calgary, Alberta, Canada. E-mail: ccbarnab@ucalgary.ca

Diagnostic imaging plays a prominent role in the diagnosis and monitoring of disease progression in arthritis conditions. Plain radiography, magnetic resonance imaging (MRI), and ultrasound (US) dominate the current field and provide complementary information on the degree of both active and chronic changes[1]. Computed tomography (CT), however, remains the best modality to assess bone[2]. High-resolution peripheral quantitative computed tomography (HR-pQCT; Scanco Medical AG) is a technical modification of conventional CT designed to examine bone microarchitecture and density, allowing visualization and quantification of the separate behavior of trabecular and cortical bone structures[3]. This technology has been validated for the examination of systemic bone density and microstructure at the distal radius and tibia in osteoporosis research[4].

Recent efforts have been made to use HR-pQCT to assess periarticular bone changes in a variety of arthritis conditions including rheumatoid arthritis (RA) and psoriatic arthritis

(PsA), and in normal states. This research has been facilitated under the auspices of the SPECTRA Collaboration (Study grouP for xtrEme Computed Tomography in Rheumatoid Arthritis), an international collective of researchers in engineering, physics, and rheumatology who pursue development of periarticular image acquisition standards[5], image interpretation and analysis guides, and applications in clinical research. Because the body of literature has grown substantially, there is a need to summarize findings. The purpose of this systematic review was to (1) summarize periarticular findings at the metacarpophalangeal (MCP) and wrist joints in different types of arthritis and in the normal state; (2) assemble the literature reporting on the ability of HR-pQCT to detect findings relative to other imaging modalities; and (3) collate results on the reproducibility of image interpretation.

MATERIALS AND METHODS

Search strategy. Assisted by a research librarian, US National Library of Medicine Medical Subject Heading (MeSH) terms, keywords, and acronyms for HR-pQCT were selected. We combined this search with MeSH terms, keywords, and acronyms for the metacarpophalangeal joints (MCP) and/or wrists, to specify the periarticular regions of interest in this new application of the imaging modality (search terms, Appendix 2). PubMed (1966–April 2015), Embase (1980–April 2015), and Medline (1946–April 2015) searches were conducted to identify potentially relevant studies. Filters were applied to eliminate animal studies and identify English language studies. We did not specify by disease, to identify studies in both normal state and in a variety of arthritis conditions. A hand search of conference abstracts (American College of Rheumatology, European League Against Rheumatism, Canadian Rheumatology Association, American Society for Bone and Mineral Research) was also performed, and references from identified articles were checked manually.

Inclusion criteria. Any studies reporting original results of HR-pQCT imaging of the MCP and/or wrist joints were selected through the title/abstract search. These studies could report on normal state or any arthritis conditions [including RA, osteoarthritis (OA), PsA], as well as "pre-arthritis" states [e.g., persons positive for anticitrullinated protein antibodies (ACPA) with arthralgias]. At the full text review stage, we selected articles for data extraction if they reported on any of the following outcomes: (1) pathology findings, determined *a priori* to include bone mineral architecture, bone mineral density (BMD), erosions, vessel channels, cortical breaks, joint space, osteophytes, or surface changes; (2) comparison to other radiography; and (3) reproducibility. Article selection and data extraction were performed by 2 authors (SN and CB). If data from the same study were reported in multiple abstracts, or subsequently published, the full manuscript was preferentially used for data extraction, or the latest version of the abstract was used.

Analysis. Owing to the heterogeneity of case definitions for different pathologies, variations in analysis techniques, and the identification of studies in a variety of normal and disease states, it was not possible to perform any form of metaanalysis. Therefore, a narrative summary of the work was performed following pathology descriptions and comparisons to other radiography and reproducibility.

RESULTS

A total of 1901 unique publications was identified, each subject to selection based on the title and abstract. One hundred and thirty-six met eligibility for full-text review, with 44 selected for data extraction. Of the 44 articles, all described pathology findings, 17 related a comparison of HR-pQCT findings to another imaging modality, and 24 described precision or reproducibility (Figure 1). The studies meeting inclusion criteria are detailed in Table 1[6-15,16-25,26-35,36-45,46-49].

Pathology

Bone microarchitecture. Kolling, *et al*[47] and Feehan, *et al*[30] studied healthy volunteers only. Kolling, *et al* found that cortical thickness (CtTh) was higher at the phalangeal base compared to the metacarpal head of the MCP joint. Feehan, *et al*'s study objective was to evaluate short-term measurement precision at the metacarpal head (as well as metacarpal shaft and ultra-ultra-distal radius). Mean (SD) values for the ratio between bone volume and total volume (BV/TV), CtTh, cortical porosity, trabecular number (TbN), trabecular thickness (TbTh), and trabecular separation (TbSp) were calculated from 10 individuals for the second and third metacarpal heads. Kleyer, *et al* scanned ACPA-positive and -negative individuals without clinical symptoms of inflammatory arthritis[17]. The BV/TV was significantly reduced in ACPA+ individuals [mean 17.2 (SEM 0.6)% vs mean 20.4 (SEM 0.4)%, respectively]. Quantitative analysis of trabecular variables showed no significant differences between ACPA+ and ACPA– individuals, although a trend toward thinner trabeculae was observed in the ACPA+ group. The CtTh was significantly lower in the ACPA+ group compared to the ACPA– group (mean 0.22 vs 0.32 mm, respectively).

Five cross-sectional studies compared bone microarchitecture between subjects with RA and controls, with variable findings (Table 2). Of 3 studies assessing BV/TV, one found it to be higher in RA[27], whereas it was lower in RA subjects compared to controls in the other 2 studies[10,39]. TbTh was higher in RA subjects in 1 study[27], lower in RA subjects in 2 studies[39,46], and not different from controls in 1 study[10]. TbN was higher in RA subjects in 1 study[27], lower in RA subjects in 1 study[10], and not different in 2 studies[39,46]. TbSp and TbSpSD were higher in RA subjects in 1 study[10] but not different in the others[27,39,46]. In 2 studies each, CtTh was lower in RA subjects[27,39] and comparable to controls[10,46].

Two studies reporting longitudinal evaluation of bone microarchitecture have been reported. One study of early inflammatory arthritis patients receiving first-line therapy did not find significant changes in quantitative values obtained[8]. Töpfer, *et al* selected 5 different texture variables calculated directly from grey value images including global and local inhomogeneity, local anisotropy, variogram slope, and entropy, which are dependent on trabecular architecture in a study of erosions[9]. At baseline, no significant differences for any of the texture variables were found, when comparing erosions that eventually progressed, regressed, or remained stable.

Bone mineral density. Studies by Kolling, *et al*[47] and Feehan, *et al*[30] of healthy volunteers have evaluated BMD. Kolling,

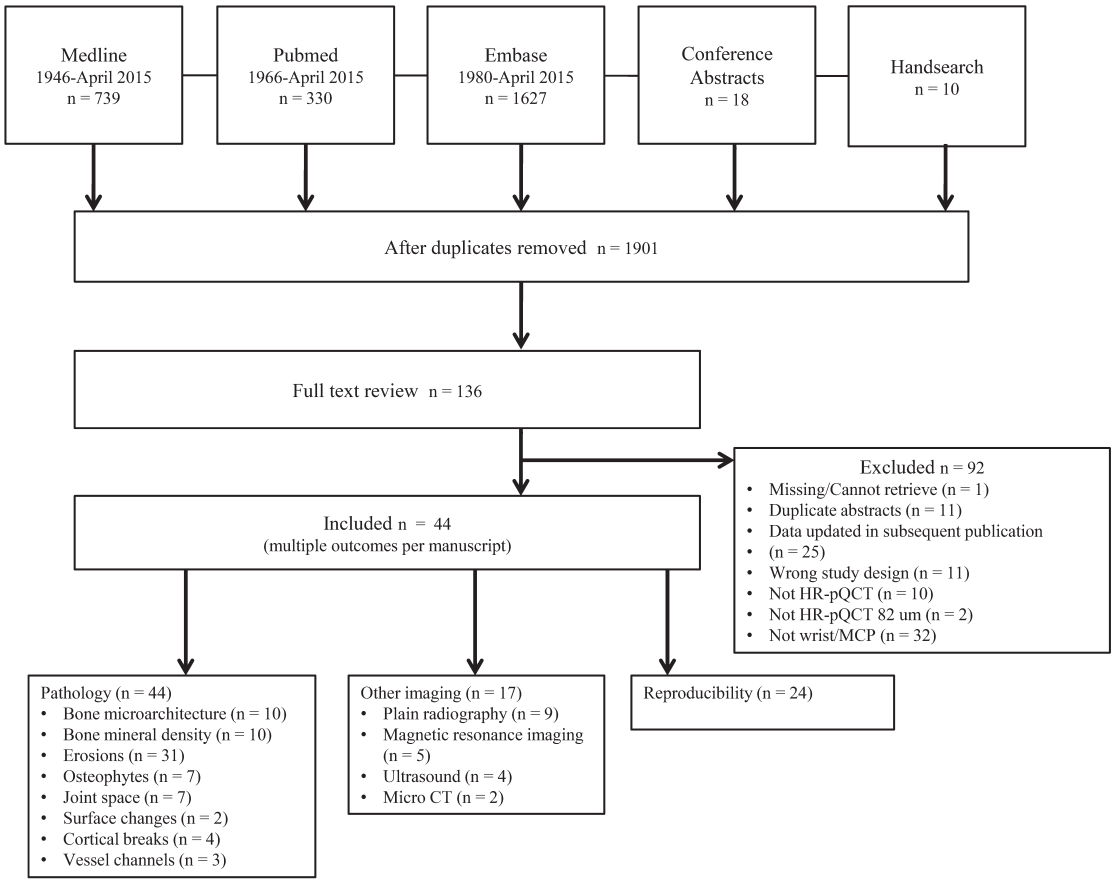

Figure 1. Flow diagram for study inclusion. HR-pQCT: high-resolution peripheral quantitative computed tomography; MCP: metacarpophalangeal (joint).

et al reported that the whole (volumetric) BMD (vBMD) increased in the distal region of the MCP, and decreased in value from the second MCP to the fourth MCP[47]. The study by Feehan, *et al* provides normative means for vBMD, as well as cortical (CtBMD) and trabecular (TbBMD) compartments at the second and third MCP[30]. Kleyer, *et al*'s study in ACPA+ and ACPA– individuals without features of inflammatory arthritis found that vBMD was significantly reduced in ACPA+ individuals (mean 280 vs 327 mg/cm^3)[17]. In studies comparing vBMD in RA subjects to controls, all found lower vBMD in RA[10,46] except for one[27]. Barnabe, *et al*[27], Yang, *et al*[10], and Fouque-Aubert, *et al*[46] found no difference between RA subjects and controls for CtBMD, whereas Zhu, *et al*[39] reported it to be significantly lower in RA. For TbBMD, Barnabe, *et al* reported it to be higher in RA subjects[27], whereas it was lower in late RA subjects only in the study by Fouque-Aubert[46], *et al*, and at the third MCP only in the Yang, *et al* study[10], but significant in the Zhu, *et al* study[39].

In a longitudinal study of changes during 1 year of therapy in early inflammatory arthritis, no significant changes were detected[8]. Two studies investigated associations between erosions and BMD measures, in particular periarticular regions of interest. In Toepfer, *et al*[51], the percent change in erosion volume correlated significantly with the percent change in BMD. In a more detailed assessment in 2015, it was found that BMD in the immediate vicinity of an erosion was significantly higher than further away from the erosion, perhaps reflecting repair mechanisms[9].

Erosions. Thirty-one publications characterizing erosions were found (Table 3). Erosions have been assessed in a variety of arthritis conditions including early inflammatory arthritis, RA, PsA, and erosive hand OA, as well as in persons with psoriasis and healthy controls, and subjects with ACPA antibodies but no features of arthritis. The case definitions used for erosions have also varied; some have required only a break in the cortical shell[9] whereas others have specified a minimum number of consecutive slices and planes with cortical breaks, but also requiring changes to be found in the trabecular bone[11]. Differences in the frequency of erosions likely reflect the underlying disease state (Table 3). In RA, a predilection for the second MCP joint, and in particular for the metacarpal head and radial side of the joint, is consistently noted[16,33,35,48]. However, in PsA, involvement of the phalangeal base and palmar surface is more common[42].

Table 1. Studies included in the systematic review.

Author, year[Ref]	Participants	Type of Study	Joints Included	Outcomes	Type of Publication
Lee, 2015[6]	RA (n = 16)	Cohort	Wrist, MCP2–3	Erosions, other radiography	Full-length report
Regensburger, 2015[7]	RA (n = 103)	Cross-sectional	MCP2–3	Erosions, other radiography, reproducibility	Full-length report
Tom, 2015[8]	EIA (n = 47)	Cohort	MCP2–3	BMA, BMD, erosions, joint space, other radiography	Abstract
Töpfer, 2015[9]	RA (n = 22)	Cohort	MCP2–4	BMA, BMD, erosions, reproducibility	Full-length report
Yang, 2015[10]	RA (n = 12); control (n = 6)	Cross-sectional	MCP2–3	BMA, BMD	Full-length report
Barnabe, 2014[11]	RA and controls, n = 58 joints	Cross-sectional	MCP2–3	Erosions, reproducibility	Abstract
Barnabe, 2014[12]	Cadaver (n = 6)	Cross-sectional	MCP2–3	Joint space	Abstract
Barnabe, 2014[13]	RA (n = 9)	Cohort	MCP2–3	Erosions, reproducibility	Abstract
Finzel, 2014[14]	PsA (n = 25); OA (n = 25)	Cross-sectional	MCP2–4	Osteophytes, reproducibility	Full-length report
Haschka, 2014[15]	ERA (n = 10); control (n = 10)	Cross-sectional	MCP2	Vessel channels	Abstract
Hecht, 2014[16]	RA (n = 267)	Cross-sectional	MCP2–4	Erosions, reproducibility	Full-length report
Kleyer, 2014[17]	ACPA+ but no history of arthritis and no signs of arthritis (n = 15); ACPA– (n = 15)	Cross-sectional	MCP2–4	BMA, BMD, erosions, cortical breaks	Full-length report
Scharmga, 2014[18]	Unknown history/ cadaver (n = 8)	Cross-sectional	MCP (not specified)	Erosions, cortical breaks, other radiography, reproducibility	Abstract
Simon, 2014[19]	PsO (n = 55); control (n = 47)	Cross-sectional	MCP2–3	Erosions, osteophytes	Abstract
Simon, 2014[20]	PsO (n = 55)	Cross-sectional	MCP2–3	Erosions, osteophytes, other radiography	Abstract
Simon, 2014[21]	PsO (n = 56); healthy (n = 24)	Cross-sectional	MCP2	Vessel channels, reproducibility	Abstract
Teruel, 2014[22]	RA (n = 16)	Cross-sectional	Wrist	Other radiography	Full-length report
Töpfer, 2014[23]	RA (n = 18)	Cross-sectional	MCP2–4	Erosions, reproducibility	Full-length report
Albrecht, 2013[24]	RA (n = 50)	Cross-sectional	MCP2–4	Erosions, other radiography, reproducibility	Full-length report
Aschenberg, 2013[25]	RA (n = 40)	Cohort	MCP2–3	Erosions, osteophytes, reproducibility	Full-length report
Barnabe, 2013[26]	ERA (n = 10)	Cross-sectional	MCP2–3	Joint space, reproducibility	Abstract
Barnabe, 2013[27]	RA (n = 15); control (n = 15)	Cross-sectional	MCP2–5 for joint space, MCP2–3 for BMA and BMD	BMA, BMD, erosions, joint space, other radiography, reproducibility	Full-length report
Boutroy, 2013[28]	Healthy (n = 6)	Cross-sectional	MCP2	Joint space, reproducibility	Abstract
Burghardt, 2013[29]	RA (n = 16); control (n = 7)	Cross-sectional	MCP2–4	Joint space, other radiography, reproducibility	Full-length report
Feehan, 2013[30]	Healthy (n = 10)	Cohort	MCP2–3	BMA, BMD, reproducibility	Full-length report
Finzel, 2013[31]	RA (n = 27); control (n = 20)	Cross-sectional	Wrist	Cortical breaks, erosions, other radiography	Abstract
Finzel, 2013[32]	RA (n = 27);Finzel, 2013[33] RA (n = 20)	Cohort	MCP2–4	Erosions, repro-ducibility	Full-length report
Finzel, 2013[34]	PsA (n = 41); RA (n = 43)	Cohort	MCP2–4	Erosions, osteophytes, reproducibility	Full-length report
Srikhum, 2013[35]	RA (n = 16), healthy (n = 7 all MCP, n = 3 wrist)	Cross-sectional	Wrist, MCP2–3	Erosions, other radiography, reproducibility	Full-length report
Toepfer, 2013[36]	RA (n = 25)	Cross-sectional	MCP2–4	Erosions, reproducibility	Abstract
Toepfer, 2013[37]	RA (n = 17)	Cohort	MCP2–4	Erosions, BMD	Abstract
Williams, 2013[38]	Unknown history/ cadaver (n = 5)	Cross-sectional	MCP (also PIP and DIP, data not separated out)	Cortical breaks, other radiography	Abstract
Zhu, 2013[39]	RA (n = 56); control (n = 56)	Cross-sectional	MCP2	BMA, BMD	Abstract
Toepfer, 2012[40]	RA (n = 18)	Cross-sectional	MCP2–4	Erosions, reproducibility	Abstract
Finzel, 2011[41]	RA (n = 26); control (n = 17)	Cross-sectional	MCP2–5	Cortical breaks, other radiography, erosions	Abstract
Finzel, 2011[42]	PsA (n = 30); RA (n = 58)	Cross-sectional	MCP2–4	Erosions, osteophytes, vessel channels, surface changes	Full-length report
Finzel, 2011[43]	RA (n = 25); PsA (n = 25); EHOA (n = 25)	Cross-sectional	MCP2–4	Erosions, joint space	Abstract
Finzel, 2011[44]	RA (n = 14); PsA (n = 6); control (n = 6)	Cross-sectional	MCP2–4	Erosions, other radiography	Full-length report
Finzel, 2011[45]	RA (n = 51)	Cohort	MCP2–4	Erosions, reproducibility	Full-length report
Fouque-Aubert, 2010[46]	RA (n = 93); control (n = 43)	Cross-sectional	MCP2–3	BMA, BMD, erosions, other radiography, reproducibility	Full-length report
Kolling, 2010[47]	Healthy (n = 19)	Cross-sectional	MCP	BMA, BMD	Abstract
Stach, 2010[48]	RA (n = 58); control (n = 30)	Cross-sectional	Wrist, MCP2–4	Erosions, osteophytes, surface changes, reproducibility, other radiography	Full-length report
Stach, 2009[49]	RA (n = 60), control (n = 30)	Cross-sectional	MCP2–3	BMA, erosions, other radiography	Abstract

RA: rheumatoid arthritis; MCP: metacarpophalangeal joints; BMD: bone mineral density; BMA: bone microarchitecture; ERA: early rheumatoid arthritis; JSW: joint space width; PsA: psoriatic arthritis; EHOA: erosive hand osteoarthritis; OA: osteoarthritis; PsO: psoriasis; EIA: early inflammatory arthritis; ACPA: anticitrullinated protein antibodies; PIP: proximal interphalangeal joints; DIP: distal IP joints.

Table 2. Comparison of bone microarchitecture (BMA) findings between rheumatoid arthritis (RA) subjects and controls.

Author[Ref]	BMA Measures Higher in RA Subjects vs Controls	BMA Measures Lower in RA Subjects vs Controls	BMA Measures Comparable between RA Subjects and Controls	Note
Stach[49]	NR	NR	NR	Cortical bone changes were evident in RA but direction and measures not specified
Fouque-Aubert[46]	NR	TbTh	TbN, TbSp, TbSpSD, CtTh	
Zhu[39]	NR	BV/TV, Ct Area, CtTh, TbTh	Tb Area, TbN, TbSp	
Barnabe[27]	BV/TV, TbTh, TbN	CtTh	TbSp	
Yang[10]	TbSp, TbSpSD	BV/TV, TbN	CtTh, CtPm, TbTh	

NR: not reported; TbTh: trabecular thickness; TbN: trabecular number; TbSp: trabecular spacing; TbSpSD: standard deviation, trabecular spacing; CtTh: cortical thickness; BV/TV: bone volume/total volume ratio; Ct area: Cortical area; Tb area: trabecular area; CtPm: cortical perimeter.

A variety of methods to describe erosion size have been proposed, including semiquantitative scores[6,48], different approaches to determining erosion volume[23,46], sphericity and surface area[9,36], and most commonly, direct measurements of the width of the cortical break and depth of trabecular loss[11]. Eight studies have reported longitudinal changes in the number and/or size of erosions[8,9,13,25,37], with some comparing changes with different therapies[33,34,45]. A small number of articles have characterized osteosclerosis of erosions in relationship to change in size with therapy[7,33,45], and 1 article described cystic bone lesions in erosive hand OA[43]. Detailed summaries of these characterizations appear in Table 3.

Vessel channels. Simon, *et al* studied subjects with cutaneous psoriasis in the investigation of bone microstructural changes prior to the onset of joint involvement, in comparison to healthy controls[21]. Patients with psoriasis had significantly more vessel channels (mean 10.8 vs 4.1) at the second metacarpal head. Similarly, more vessel channels were seen in patients with RA compared to healthy controls (mean 4.6 vs 2.3) in a study by Haschka, *et al*[15]. Cortical breaks were found in 93% of patients with PsA and 87.5% of patients with PsA in an earlier study reported by Finzel, *et al*[42].

Cortical breaks. Two studies of RA subjects[31,41], 1 study of ACPA+ and ACPA– individuals without inflammatory arthritis[17], and 1 cadaver study[38] have reported on cortical breaks; the former 3 studies used a definition of a break in the cortical lining detectable in 2 perpendicular planes with no size specification, whereas the latter used a minimum break size of > 0.5 mm[38]. In both Finzel, *et al* 2012 and Finzel, *et al* 2011, mean longitudinal and transverse width and depth dimensions of the breaks, relative to controls, were summarized[31,41]. Kleyer, *et al* found significantly more breaks in ACPA+ individuals compared to ACPA– (mean 7.4 vs 1.0 breaks, not specified whether total or per joint)[17]. The Williams, *et al* study included MCP as well as proximal and distal interphalangeal joints without separating the results at each region, and found 35 breaks in 13 joints[38].

Joint space. Several approaches to measuring joint space have been proposed. Barnabe, *et al* used region-growing image processing in a study of RA subjects matched to healthy controls, finding that MCP were narrowed in the RA group[27]. In further studies by this group, a custom script applying the approach of "fitting maximal spheres" was applied to estimate mean joint space width in early inflammatory arthritis[26], and also in a cadaver study examining changes in mean, median, minimum, and maximum joint space widths and total volume estimates based on angle of positioning[12]. They also applied this script in assessing treatment effect over 1 year in early inflammatory arthritis, seeing improved/increased joint space at the second MCP[8]. Burghardt, *et al* applied a method of voxel counting for joint space volume and a 3-D distance transformation method for morphology also using a method of "fitting of maximal spheres" to examine joint space mean, minimum, maximum, asymmetry, and SD in RA and healthy controls[29]. RA subjects had a smaller joint space minimum compared to the control group, but without significant differences found for the other variables[29]. Burghardt, *et al* also examined the wrist, finding a higher SD of the radiolunate and radioulnar joints in RA subjects, with lower minimum measurement in the radiolunate joint but higher maximum, indicating asymmetry[29]. Boutroy, *et al* has also developed an automated algorithm, but technical specifications were not provided[28]. In an abstract by Finzel, *et al* comparing RA, PsA, and erosive hand OA, joint space narrowing was measured using a manual technique at medial, lateral, and middle aspects of the joint; however, age, sex, and postmenopausal state were associated with joint space narrowing in the OA subjects[43].

Osteophytes. Seven studies, all from the same research group, have applied a definition of osteophytes as bony protrusions from the juxtaarticular cortical shell. In the original publication of RA subjects and healthy controls, osteophytes were described as being small and located at the dorsal and palmar aspects of the joint, with similar frequency of occurrence in the 2 groups and correlating with subject age[48]. In a 1-year followup study of RA subjects, osteophytes increased in both quantity and size[25]. Patients with PsA were described as having a more significant osteophyte burden relative to RA. In the study by Finzel, *et al* in 2011, 16% of RA but 100% of

The Journal of Rheumatology 2016; 43:10; doi:10.3899/jrheum.160647

Table 3. Publications characterizing erosions using HR-pQCT.

Author[Ref]	Participants	Erosion Definition	Frequency	Location	Size	Longitudinal Assessment	Shape	Other Features Described
Lee[6]	RA (n = 16)	Sharply demarcated juxtaarticular focal bone lesion with a cortical break (loss of cortex) in at least 2 adjacent slices	94%; mean 5.4/patient (MCP2, 3)	NR	Width, semi-quantitative score	NR	NR	
Tom[8]	EIA (n = 47) but only 27 with 1-year followup	SPECTRA*	23%	NR	Width and depth in axial and perpendicular axes	1 year (n = 27): 56% no erosions; 7% erosions resolved; 22% erosion no. stable; 15% erosion no. increased. Increases in mean size for all dimensions except perpendicular width, which decreased; few progressed > SDC	NR	
Töpfer[9]	RA (n = 22)	Juxtaarticular break in the cortical shell	N = 40; 12 subjects single erosion, 10 subjects multiple erosions	NR	Sphericity, volume	20% decreased and 15% increased in volume	NR	
Barnabe[11]	RA and controls, n = 58 joints	SPECTRA	NR	NR	Width and depth in axial and perpendicular axes	NR	NR	
Barnabe[13]	RA (n = 9)	SPECTRA	NR	NR	Width and depth in axial and perpendicular axes	1 year: 1 new erosion. No significant change in erosion dimensions	NR	
Hecht[16]	RA (n = 267)	Pathological cortical break within bone lining	N = 897; 25% of subjects had no erosions. Mean 5.4/RF+ACPA+ patient and mean 2.5/RF–ACPA– patient (all MCP)	MCP2 most commonly affected	Width, depth, volume	NR	NR	
Kleyer[17]	ACPA+ but no history of arthritis and no signs of arthritis (n = 15); ACPA– (n = 15)	Juxtaarticular break in the cortical shell	N = 5 in ACPA+, N = 5 ACPA–	Radial aspect of 2nd and 3rd MCP most commonly affected in both groups	Width, depth	NR	NR	
Scharmga[18]	Unknown history/cadaver (n = 8)	SPECTRA	N = 24 Mean 1.3/joint	NR	NR	NR	NR	
Simon[19]	PsO (n = 55); control (n = 47)	Cortical breaks within the joint and visible in 2 planes	N = 27 in PsO, N = 18 in controls	Most frequent location of erosions was radial aspect of MCH 2 in both groups	Volume	NR	NR	
Simon[20]	PsO (n = 55)	NR	29%	NR	NR	NR	NR	
Töpfer[23]	RA (n = 18)	Not specified	N = 43, mean 2.4/patient (MCP2, 3, 4)	NR	NR	NR	NR	
Albrecht[24]	RA (n = 50)	Juxtaarticular break in the cortical shell	Erosions found in 137/600 of evaluated joint regions	NR	Volume	NR	NR	
Aschenberg[25]	RA (n = 40)	Juxtaarticular break in the cortical shell	Mean 5.7/subject (MCP2, 3)	NR	Semiquantitative score	1 year: Increase to 6.13/subject and in erosion score	NR	

Table 3. Continued

Author[Ref]	Participants	Erosion Definition	Frequency	Location	Size	Longitudinal Assessment	Shape	Other Features Described
Barnabe[27]	RA (n = 15); control (n = 15)	Definite cortical break on a 2–dimensional image extending over a minimum of three 82-micron slices	RA: 100%, mean 23.6/subject; controls: 60%, mean 3.6/subject (All PIP and MCP evaluated)	RA: MCH > PB; controls: PIP > MCP	NR	NR	NR	
Finzel[31]	RA (n = 27); control (n = 20)	Cortical break defined as defect in cortical lining detectable in 2 perpendicular planes. Physiological and abnormal breaks defined according to examiner	NR	wrist	Width and depth in axial and perpendicular axes	NR	NR	
Finzel[32]	RA (n = 27); control (n = 20)	Cortical break defined as defect in cortical lining detectable in 2 perpendicular planes. Physiological and abnormal breaks defined according to examiner	NR	MCP	Width and depth in axial and perpendicular axes	NR	NR	
Finzel[33]	RA (n = 20)	Break of the juxtaarticular cortical bone	N = 133	MCP2 > MCP3, 4; MCH > PB; radial > ulnar, palmar or dorsal	Width, depth	1 year: 9 new erosions. Width of bone erosions significantly decreased with TCZ	NR	Osteosclerosis determined in relation to change in erosion size
Finzel[34]	PsA (n = 41); RA (n = 43)	NR	NR	NR	Width, depth	Width of erosions did not progress in MTX- or TNFi-treated PsA patients	NR	
Regensburger[7]	RA (n = 103)	Clear juxtaarticular bone lesion with a cortical break that can be seen in 2 consecutive images in 2 perpendicular planes	N = 360	NR	NR	NR	NR	Osteosclerosis
Srikhum[35]	RA (n = 16); healthy (n = 7)	Sharply demarcated juxtaarticular focal bone lesion with (loss of cortex) in at least 2 adjacent slices	RA (n = 30); MCP2, 69%; MCP3, 50%; controls (n = 3); MCP2 29%; MCP3 43%	MCP2 > MCP3	Axial width a cortical break	NR MCP3, 50%;	NR	
Toepfer[36]	RA (n = 25)	NR	NR	NR	Volume, sphericity, surface area	NR	NR	
Toepfer[37]	RA (n = 17)	NR	N = 37	NR	Volume	1 year: change in erosion volume correlated significantly with change in BMD	NR	

Table 3. Continued

Author[Ref]	Participants	Erosion Definition	Frequency	Location	Size	Longitudinal Assessment	Shape	Other Features Described
Toepfer[40]	RA (n = 18)	NR	N = 32	NR	Volume	NR	NR	
Finzel[41]	RA (n = 26); control (n = 17)	Distinguished from cortical breaks if they are "abnormal"	NR	NR	Width and depth in axial and perpendicular axes	NR	NR	
Finzel[42]	PsA (n = 30); RA (n = 58)	Juxtaarticular break in the cortical shell	PsA 93%, RA 88%; mean 6.3/PsA patient and 6.1/RA patient (MCP2, 3, 4)	RA and PsA: MCP2 and MCP3 > MCP4; RA: radial > ulnar, palmar, dorsal; PsA: palmar and phalangeal base affected > RA	Width, depth, semi-quantitative score	NR	U-shaped RA 86%, PsA 39%; omega-shaped PsA 68%; T-shaped PsA 36%, RA 5%	
Finzel[43]	RA (n = 25); PsA (n = 25) EHOA (n = 25)	NR	No. bone erosions similar in RA, PsA, and EHOA	EHOA: Ulnar and radial MCH > PB	RA erosion size > PsA and EHOA (not specified)	NR	NR	Cystic bone lesions
Finzel[44]	RA (n = 14); PsA (n = 6); control (n = 6)	Juxtaarticular break in the cortical shell	NR	Radial MCP2 most commonly affected; MCP2, 3 > MCP4	Severity (not specified)	NR	NR	
Finzel[45]	RA (n = 51)	Juxtaarticular break in the cortical shell	N = 72 TNFi group, N = 55 MTX group	NR	Width, depth	1 year: mean depth significantly decreased with TNFi; mean width and depth significantly increased with MTX	NR	Osteosclerosis and lesion depth determined in relation to change in erosion size
Fouque-Aubert[46]	RA (n = 93); control (n = 43)	Sharply marginated bone lesions with juxtaarticular localization with a cortical break seen in at least 2 adjacent slices	MCP2 27%, MCP3 23%	NR	Volume	NR	NR	
Stach[48]	RA (n = 58); control (n = 30)	Juxtaarticular break in the cortical shell	RA 84%, controls 37%	RA: radial > ulnar, palmar, dorsal; MCP2,3 > MCP4; MCH > PB	Width, depth	NR	NR	
Stach[49]	RA (n = 60); control (n = 30)	NR	RA frequent discontinuities of the cortical surface, virtually absent in healthy subjects.	NR	Size (not specified)	NR	NR	

*SPECTRA Collaboration: Presence of a cortical break extending over at least 2 slices and seen in 2 orthogonal views. The break must be nonlinear in shape to differentiate from vascular channels penetrating the cortical surface and have underlying trabecular bone loss. Frequency: n = refers to no. erosions unless specified as % of subjects or mean no. erosions per subject or surface. NR: not reported; SDC: smallest detectable change; MCH metacarpal head; PB: phalangeal base; MCP: metacarpophalangeal joint; PIP: proximal interphalangeal joint; TCZ: tocilizumab; MTX: methotrexate; TNFi: tumor necrosis factor inhibitors; PsA: psoriatic arthritis; RA: rheumatoid arthritis; EHOA: erosive hand osteoarthritis; BMD: bone mineral density; EIA: early inflammatory arthritis; ACPA: anti-citrullinated protein antibodies; PsO: psoriasis; RF: rheumatoid factor; HR-pQCT: high-resolution peripheral quantitative computed tomography.

PsA subjects had osteophytes, predominantly located at the second and third MCP rather than the fourth MCP[42]. The mean number of osteophytes was 11.6 in PsA but only 2.1 in RA, with a mean size of 1.2 mm in PsA versus 0.5 mm in RA[42]. Also, in RA the osteophytes were predominantly located at the dorsal and palmar aspects of the joint, but those in PsA were located at all aspects and appeared as a bony corona[42]. In a 1-year longitudinal study of patients with PsA treated with antitumor necrosis factor or methotrexate therapy, osteophytes significantly progressed in size in both treatment groups; and with an RA comparison group there was a similar finding[34]. A comparison between PsA and hand OA has been performed[14]. In this study, osteophytes/bone spurs were nearly universal in both conditions, but with PsA having larger spurs, and with different localizations; at the second MCP both phalangeal and metacarpal heads were more likely affected in PsA, and with a predilection for radial aspect. In hand OA it was the third MCP, with palmar and dorsal quadrants affected[14]. Also in PsA, spurs in entheseal regions were prominent, whereas in OA these were emerging at the cartilage/bone interface and the joint margin[14]. In psoriasis, 1 abstract describes a population of 55 subjects, all of whom were found to have osteophytes but without further characterization[20]. One cross-sectional study compares psoriasis patients and healthy controls, with more frequent bony spurs in psoriasis, most commonly located at the second metacarpal head, but being larger in size in psoriasis subjects[19].

Surface changes. Using 3-D reconstruction images of the bone surface, alterations of cortical thinning and fenestration but not breaks have been characterized. Surface changes predominated in PsA relative to RA (93% vs 79% of patients had surface changes, respectively) but the extent of the changes was similar between diseases[42]. Another finding was that of lesser lesion severity at the fourth MCP in PsA compared to RA, whereas these were similar at the second and third MCP[42]. Controls had small areas of these changes relative to RA subjects[48].

Comparison to other radiographic modalities. Seventeen individual publications have compared findings on HR-pQCT to other imaging modalities, including plain radiography, MRI, power Doppler US, high-resolution US, and *ex-vivo* micro-CT scans, and predominantly for erosion detection but also in correlating findings of inflammation (primarily by MRI) and joint space narrowing. In an abstract, Stach and Schett reported a sensitivity of 0.75 and specificity of 0.85 for HR-pQCT compared to plain radiography to detect small bone erosions[49]. This abstract was followed by a full publication that reported that 58% of patients with lesions on HR-pQCT had normal radiographs, and that no patient with lesions on radiographs had a normal HR-pQCT scan[48]. Similarly, authors comparing erosion detection by plain radiography and HR-pQCT have found HR-pQCT to have increased sensitivity[8,18,27,38,46]. HR-pQCT has been used in further studies as the gold standard for erosions relative to MRI[6,7,24,35], power Doppler US[31,32,33], high-resolution US[44], and plain radiography[6]. Simon, *et al* reported poor correlation between bony changes seen in HR-pQCT scans with osteitis and synovitis seen on MRI in patients with psoriasis[20]. A single study has compared plain radiography scored by the van der Heijde modified Sharp method and an HR-pQCT joint space width measurement algorithm[29]. Joints with radiographic narrowing had higher joint space heterogeneity and less than half the minimum joint space width on HR-pQCT compared to joints without radiographic narrowing[29].

Reproducibility. Reproducibility metrics for inter- and intrarater readings, repositioning, scan/re-scan, and contouring reproducibility have been reported for measures of bone microarchitecture and BMD, erosion and osteophyte characterization, and joint space width (Table 4).

Intraclass correlation coefficients (ICC) for inter- and intrarater assessments of bone microarchitecture exceeded 0.9[17], whereas scan/re-scan coefficients of variation (CV) ranged up to 12.5%[30,46]. The root mean square CV (RMSCV) for contouring reproducibility was < 0.8%[27]. The RMSCV for BMD measures for intra- and interrater were < 3.3%[40], and scan/re-scan and contouring reproducibility were excellent[27,30,46]. Good interrater agreement for erosion detection and count has been reported by most authors[7,11,13,16,24,25]. In general, good values for interrater determination of erosion size were obtained, with excellent intrarater ICC[9,11,13,33,35,45]. There is evidence for variations in joint space width measurements related to repositioning and scan/re-scan[26,28,29].

DISCUSSION

This systematic review serves as a comprehensive narrative summary of the available literature on the use of HR-pQCT imaging of the periarticular bone of the MCP or wrists. Despite HR-pQCT being available for only about 10 years, there is considerable literature on its use in imaging of MCP or wrists to describe findings in early inflammatory arthritis, RA, PsA, erosive hand OA, psoriasis, "pre-arthritis," and healthy controls. The vast majority of studies identified focus on characterizing erosions, with an apparent evolution in case definition standardization but with an ongoing need to standardize and automate methods to measure erosion dimensions. In the evaluation of erosions, other reasons for breaks in the cortical bone such as vessel channels have become apparent, with further studies required to elucidate whether these channels reflect disease pathophysiology or evolve into pathologic states. Other areas of pathology description require further development, such as defining and measuring osteophytes, and achieving consensus on methods for measuring joint space width, along with correlation to tissue studies to confirm findings. At this time standard evaluations have been applied to provide quantitative measures for bone

Table 4. Reproducibility measures.

Author	Participants	Reproducibility Feature	Findings
Bone microarchitecture measures			
Kleyer[17]	ACPA+ but no history of arthritis and no signs of arthritis (n = 15); ACPA– (n = 15)	Interrater	ICC > 0.90
Kleyer[17]	ACPA+ but no history of arthritis and no signs of arthritis (n = 15); ACPA– (n = 15)	Intrarater	ICC > 0.95
Fouque-Aubert[46]	RA (n = 93); control (n = 43)	Repositioning and scan/rescan	CV 2.9–12.5%
Feehan[30]	Healthy (n = 10)	Scan/rescan	ICC > 0.884, CV < 4.8%, RMSCV < 6.2%
Barnabe[27]	RA (n = 15); control (n = 15)	Contouring reproducibility*	RMSCV < 0.8%
Bone mineral density			
Töpfer[23]	RA (n = 18)	Interrater	RMSCV < 3.1%
Töpfer[23]	RA (n = 18)	Intrarater	RMSCV < 3.3%
Feehan[30]	Healthy (n = 10)	Scan/rescan	ICC > 0.975, CV < 1.5%, RMSCV < 2.1%
Fouque-Aubert[46]	RA (n = 93); control (n = 43)	Repositioning and scan/rescan	CV < 1.8%
Barnabe[27]	RA (n = 15); control (n = 15)	Contouring reproducibility*	RMSCV < 0.8%
Cortical break count			
Simon[21]	PsO (n = 56); healthy (n = 24)	Interrater	r = 0.96
Scharmga[18]	Unknown history/cadaver (n = 8)	Intrarater	ICC 0.399
Simon[21]	PsO (n = 56); healthy (n = 24)	Intrarater	r = 0.98
Erosion detection			
Barnabe[11]	RA and controls (n = 58 joints)	Interrater	Agreement 90.2%
Barnabe[13]	RA (n = 9)	Interrater	Agreement 92.9%; κ = 0.711, 95% CI 0.539–0.839
Regensburger[7]	RA (n = 103)	Interrater	κ = 0.975
Erosion count			
Albrecht[24]	RA (n = 50)	Interrater	ICC range 0.936–1.00
Hecht[16]	RA (n = 267)	Interrater	ICC range 0.872–1.000
Regensburger[7]	RA (n = 103)	Interrater	ICC 0.979 (95% CI 0.976–0.982)
Scharmga[18]	Unknown history/cadaver (n = 8)	Intrarater	ICC 0.142
Aschenberg[25]	RA (n = 40)	Interrater*	ICC mean 0.79; range 0.57–0.95
Erosion size			
Barnabe[11]	RA and controls (n = 58 joints)	Interrater	RMSCV range 12.3–24%
Barnabe[13]	RA (n = 9)	Interrater	RMSCV range 15.7–36.4%
Finzel[33]	RA (n = 20)	Interrater	ICC > 0.93
Finzel[45]	RA (n = 51)	Interrater	ICC 0.95
Srikhum[35]	RA (n = 16); healthy (n = 7, all MCP, n = 3 wrist)	Interrater	ICC 0.89, RMSE 9.4%
Töpfer[9]	RA (n = 22)	Interrater	Precision error range 6.0–8.3%
Finzel[33]	RA (n = 20)	Intrarater	ICC 0.99
Finzel[45]	RA (n = 51)	Intrarater	ICC 1.0
Srikhum[35]	RA (n = 16); healthy (n = 7 all MCP, n = 3 wrist)	Intrarater	ICC 0.99, RMSE 4.7%
Erosion score			
Stach[48]	RA (n = 58); control (n = 30)	Interrater	κ = 0.75
Aschenberg[25]	RA (n = 40)	Interrater*	ICC mean 0.79; range 0.57–0.95
Stach[48]	RA (n = 58); control (n = 30)	Intrarater	κ = 0.82
Erosion sphericity			
Töpfer[23]	RA (n = 18)	Interrater	RMSCV 5.5%
Toepfer[40]	RA (n = 18)	Interrater	RMSCV 4.9%
Töpfer[23]	RA (n = 18)	Intrarater	RMSCV 2.8%
Toepfer[36]	RA (n = 25)	Intrarater	RMSCV 2.5%
Erosion surface area			
Töpfer[23]	RA (n = 18)	Interrater	RMSCV 9.9%
Toepfer[40]	RA (n = 18)	Interrater	RMSCV 10.4%
Töpfer[23]	RA (n = 18)	Intrarater	RMSCV 5.8%
Toepfer[36]	RA (n = 25)	Intrarater	RMSCV 4.7%
Erosion volume			
Regensburger[7]	RA (n = 103)	Interrater	ICC 0.951 (95% CI 0.937, 0.962)
Töpfer[23]	RA (n = 18)	Interrater	RMSCV 7.8%
Toepfer[40]	RA (n = 18)	Interrater	RMSCV 7.8%
Töpfer[23]	RA (n = 18)	Intrarater	RMSCV 5.7%
Toepfer[36]	RA (n = 25)	Intrarater	RMSCV 4.1%

Table 4. Continued.

Author	Participants	Reproducibility Feature	Findings
Joint space width			
Barnabe[27]	RA (n = 15); control (n = 15)	Contouring reproducibility	RMSCV 17.1%
Barnabe[26]	ERA (n = 10)	Repositioning	RMSCV 4.8%
Boutroy[28]	Healthy (n = 6)	Repositioning	Estimates vary with positioning at 0° and 30°; maximum increases 12.5% and mean increases 16.4%, less effect on volume, minimum, and asymmetry
Burghardt[29]	RA (n = 16); control (n = 7)	Scan/re-scan	RMSCV range 2.1–13.9%
Osteophyte measurement			
Finzel[34]	PsA (n = 41); RA (n = 43)	Interrater	r = 0.9692
Finzel[34]	PsA (n = 41); RA (n = 43)	Intrarater	r = 0.9722
Osteophyte count			
Aschenberg[25]	RA (n = 40)	Interrater* (osteophyte count)	ICC mean 0.79; range 0.57–0.95
Osteophyte score			
Aschenberg[25]	RA (n = 40)	Interrater* (osteophyte score)	ICC mean 0.79; range 0.57–0.95

*In each article, results were not separated for the different measures. PsA: psoriatic arthritis; RA: rheumatoid arthritis; BMD: bone mineral density; EIA: early inflammatory arthritis; ACPA: anticitrullinated protein antibodies; PsO: psoriasis; RF: rheumatoid factor; RMSCV: root mean square coefficient of variation; ICC: intraclass correlation coefficients; MCP: metacarpophalangeal joint; RMSE: root mean square error; ERA: early RA.

microarchitecture and BMD, although notably the region of interest to be evaluated has varied among authors, either using a set number of slices to be evaluated or a percentage of the metacarpal length to adjust for size.

HR-pQCT is frequently used as the gold standard for erosion detection relative to other imaging modalities including plain radiography, US, and MRI. The high resolution it provides also allows identification of erosive findings in unexpected states, such as in healthy controls, and further work should be directed to refining what is a naturally occurring finding, and how a pathological finding evolves. Although not able to detect soft tissue changes, limiting its abilities relative to US and MRI, HR-pQCT provides microarchitectural detail that those modalities cannot, and is useful in elucidating the evolution of joint damage and even regression of developing lesions[35].

Current assessment protocols for quantitative measures exhibit good to excellent reproducibility metrics, whether for direct or derived outcomes, or application of semiquantitative scores. There is evidence that positioning affects quantitative joint space width measures, and there is a need to ensure that a standardized positioning device or protocol be used going forward, in particular for longitudinal studies.

Our review also serves to highlight areas in which data are lacking. Very few reports have assessed the wrist joint, which is a common location for damage in most types of arthritis. Findings have not been described in other systemic inflammatory arthritis conditions such as crystal arthritis, and at a variety of disease stages for RA, PsA, and erosive hand OA. Normative data have been collected infrequently and longitudinal assessments have been rare, and both types of data would further enhance our understanding of the sensitivity of HR-pQCT imaging assessments over time. Of note, a second-generation version HR-pQCT has been released, providing 61 μm of nominal isotropic resolution in contrast to the 82 μm technology that all studies in this review have used. With higher sensitivity imaging available, resolving the determination of the relevance of findings will be important.

HR-pQCT may ultimately prove to be key in the diagnosis of arthritis conditions, and may be used in conjunction with biomarkers or other imaging modalities such as US to more accurately predict patient outcomes. As well, it could be an important tool for the longitudinal monitoring of disease activity and structural bone changes. The sensitivity of the technique may allow detection of small but significant improvements for the purposes of clinical trials for inflammatory diseases. HR-pQCT imaging can be applied in rheumatology outcomes research for the benefit of patients affected by inflammatory joint disease regarding early diagnosis, resulting in initiation of early and appropriate treatment.

APPENDIX 1.

List of study collaborators. SPECTRA Collaboration Members:
Cheryl Barnabe, University of Calgary; Susan Barr, University of Calgary; Stephanie Boutroy, Université de Lyon; Steven K. Boyd, University of Calgary; Andrew Burghardt, University of California San Francisco; Roland Chapurlat, Université de Lyon; Angela Cheung, University of Toronto; Joost de Jong, Maastricht University Medical Centre; Klaus Engelke, University of Erlangen; Lynne Feehan, University of British Columbia; Stephanie Finzel, Department of Rheumatology and Clinical Immunology, University Medical Center Freiburg, Faculty of Medicine, University of Freiburg; Piet Geusens, Maastricht University Medical Centre; Ellen-Margrethe Hauge, Aarhus University Hospital; Yebin Jiang, University of Michigan; Kresten Keller, Aarhus University Hospital; Roland Kocijan, University of Vienna; Sebastian Kraus, University of Erlangen; Xiaojuan Li, University of California San Francisco; Hubert Marotte, Université de Lyon; Liam Martin, University of Calgary; Rosa Pereira, University of Sao Paolo; Andrea Scharmga, Maastricht University Medical Centre; Georg Schett, University of Erlangen; Kristian Stengaard-Pedersen, Aarhus University Hospital;

Kathryn S. Stok, ETH Zurich; Nikolay Tzaribachev, SCANCO Medical AG; Joop van den Bergh, Maastricht University Medical Centre; Bert van Rietbergen, Eindhoven University of Technology; Astrid van Tubergen, Maastricht University Medical Centre; Mira van Veenendaal, University of Toronto; Paul Willems, Maastricht University Medical Centre; Jeroen Williams, Maastricht University Medical Centre; Rae Yeung, University of Toronto.

REFERENCES

1. Filippucci E, Di Geso L, Grassi W. Progress in imaging in rheumatology. Nat Rev Rheumatol 2014;10:628-34.
2. Perry D, Stewart N, Benton N, Robinson E, Yeoman S, Crabbe J, et al. Detection of erosions in the rheumatoid hand; a comparative study of multidetector computerized tomography versus magnetic resonance scanning. J Rheumatol 2005;32:256-67.
3. Geusens P, Chapurlat R, Schett G, Ghasem-Zadeh A, Seeman E, de Jong J, et al. High-resolution in vivo imaging of bone and joints: a window to microarchitecture. Nat Rev Rheumatol 2014;10:304-13.
4. Cheung AM, Adachi JD, Hanley DA, Kendler DL, Davison KS, Josse R, et al. High-resolution peripheral quantitative computed tomography for the assessment of bone strength and structure: a review by the Canadian Bone Strength Working Group. Curr Osteoporos Rep 2013;11:136-46.
5. Barnabe C, Feehan L. High-resolution peripheral quantitative computed tomography imaging protocol for metacarpophalangeal joints in inflammatory arthritis: The SPECTRA collaboration. J Rheumatol 2012;39:1494-5.
6. Lee CH, Srikhum W, Burghardt AJ, Virayavanich W, Imboden JB, Link TM, et al. Correlation of structural abnormalities of the wrist and metacarpophalangeal joints evaluated by high-resolution peripheral quantitative computed tomography, 3 Tesla magnetic resonance imaging and conventional radiographs in rheumatoid arthritis. Int J Rheum Dis 2015;18:628-39.
7. Regensburger A, Rech J, Englbrecht M, Finzel S, Kraus S, Hecht K, et al. A comparative analysis of magnetic resonance imaging and high-resolution peripheral quantitative computed tomography of the hand for the detection of erosion repair in rheumatoid arthritis. Rheumatology 2015;54:1573-81.
8. Tom S, Finzel S, Blair-Pattison A, Martin L, Hazlewood G, Barber C, et al. Quantified differences in erosion number and size in the first year of inflammatory arthritis using high-resolution peripheral quantitative computed tomography (HR-pQCT). J Rheumatol 2015;42:1335-6.
9. Töpfer D, Gerner B, Finzel S, Kraus S, Museyko O, Schett G, et al. Automated three-dimensional registration of high-resolution peripheral quantitative computed tomography data to quantify size and shape changes of arthritic bone erosions. Rheumatology 2015;54:2171-80.
10. Yang H, Yu A, Burghardt AJ, Virayavanich W, Link TM, Imboden JB, et al. Quantitative characterization of metacarpal and radial bone in rheumatoid arthritis using high resolution-peripheral quantitative computed tomography. Int J Rheum Dis 2015 Apr 10 (E-pub ahead of print).
11. Barnabe C, Kraus S, Marotte H, Hauge EM, Scharmga A, Kocijan R, et al. Case definition for erosions imaged with high resolution peripheral quantitative computed tomography (HR-PQCT): An international spectra reliability exercise-1 (relex-1). Ann Rheum Dis 2014;73 Suppl 2:473-4.
12. Barnabe C, Manske S, Jorgenson B, Boyd SK. Optimal hand position for reliable volumetric joint space width measurements using high-resolution peripheral quantitative computed tomography. Arthritis Rheum 2014;66:S938-9.
13. Barnabe C, Marotte H, Scharmga A, Kraus S, Burghardt A, Hauge EM, et al. Rheumatoid arthritis erosion detection and measurement in longitudinal datasets using high-resolution peripheral quantitative computed tomography (HR-PQCT): Reliability exercise-2 (relex-2). Ann Rheum Dis 2014;73 Suppl 2:654-5.
14. Finzel S, Sahinbegovic E, Kocijan R, Engelke K, Englbrecht M, Schett G. Inflammatory bone spur formation in psoriatic arthritis is different from bone spur formation in hand osteoarthritis. Arthritis Rheumatol 2014;66:2968-75.
15. Haschka J, Simon D, Rech J, Hueber AJ, Schett G, Kleyer A. In vivo detection of cortical micro channels in metacarpophalangeal joints with xtreme CT — a new instrument to visualize communication between the bone marrow and the joint space. Ann Rheum Dis 2014;73 Suppl 2:659.
16. Hecht C, Englbrecht M, Rech J, Schmidt S, Araujo E, Engelke K, et al. Additive effect of anti-citrullinated protein antibodies and rheumatoid factor on bone erosions in patients with RA. Ann Rheum Dis 2014;74:2151-6.
17. Kleyer A, Finzel S, Rech J, Manger B, Krieter M, Faustini F, et al. Bone loss before the clinical onset of rheumatoid arthritis in subjects with anticitrullinated protein antibodies. Ann Rheum Dis 2014;73:854-60.
18. Scharmga A, van Tubergen A, van den Bergh J, de Jong J, Peters M, van Rietbergen B, et al. Cortical breaks and bone erosions in the hand joints: a cadaver study comparing conventional radiography with high-resolution and micro-computed tomography. Ann Rheum Dis 2014;73 Suppl 2:650.
19. Simon D, Faustini F, Englbrecht M, Kleyer A, Kocijan R, Haschka J, et al. Bone microstructure in patients with cutaneous psoriasis and no history of psoriatic arthritis shows bone anabolic changes at a greater extent than in healthy controls. Arthritis Rheum 2014;66 Suppl 11:S931-2.
20. Simon D, Faustini F, Englbrecht M, Kleyer A, Kocijan R, Haschka J, et al. Magnetic resonance imaging (MRI) of hands of psoriasis patients: high incidence of inflammation. Ann Rheum Dis 2014;73 Suppl 2:656.
21. Simon D, Faustini F, Kleyer A, Haschka J, Werner D, Hueber A, et al. In vivo visualization of cortical microchannels in metacarpal bones in patients with cutaneous psoriasis by high resolution peripheral computed tomography - detecting cortical pathologies before the clinical onset of psoriatic arthritis [abstract]. Arthritis Rheum 2014;66 Suppl 11:S832.
22. Teruel JR, Burghardt AJ, Rivoire J, Srikhum W, Noworolski SM, Link TM, et al. Bone structure and perfusion quantification of bone marrow edema pattern in the wrist of patients with rheumatoid arthritis: a multimodality study. J Rheumatol 2014;41:1766-73.
23. Töpfer D, Finzel S, Museyko O, Schett G, Engelke K. Segmentation and quantification of bone erosions in high-resolution peripheral quantitative computed tomography datasets of the metacarpophalangeal joints of patients with rheumatoid arthritis. Rheumatology 2014;53:65-71.
24. Albrecht A, Finzel S, Englbrecht M, Rech J, Hueber A, Schlechtweg P, et al. The structural basis of MRI bone erosions: an assessment by microCT. Ann Rheum Dis 2013;72:1351-7.
25. Aschenberg S, Finzel S, Schmidt S, Kraus S, Engelke K, Englbrecht M, et al. Catabolic and anabolic periarticular bone changes in patients with rheumatoid arthritis: a computed tomography study on the role of age, disease duration and bone markers. Arthritis Res Ther 2013;15:R62.
26. Barnabe C, Buie H, Kan M, Szabo E, Barr SG, Martin L, et al. Reproducible metacarpal joint space width measurements using 3D analysis of images acquired with high-resolution peripheral quantitative computed tomography. Med Eng Phys 2013;35:1540-4.
27. Barnabe C, Szabo E, Martin L, Boyd SK, Barr SG. Quantification of small joint space width, periarticular bone microstructure and erosions using high-resolution peripheral quantitative computed tomography in rheumatoid arthritis. Clin Exp Rheumatol 2013;31:243-50.

28. Boutroy S, Hirschenhahn E, Youssof E, Locrelle H, Thomas T, Chapurlat R, et al. Importance of hand positioning in 3D joint space morphology assessment. Arthritis Rheum 2013;65 Suppl 10:S840-1.
29. Burghardt AJ, Lee CH, Kuo D, Majumdar S, Imboden JB, Link TM, et al. Quantitative in vivo HR-pQCT imaging of 3D wrist and metacarpophalangeal joint space width in rheumatoid arthritis. Ann Biomed Eng 2013;41:2553-64.
30. Feehan L, Buie H, Li L, McKay H. A customized protocol to assess bone quality in the metacarpal head, metacarpal shaft and distal radius: a high resolution peripheral quantitative computed tomography precision study. BMC Musculoskelet Disord 2013;14:367.
31. Finzel S, Aergeter P, Schett G, D'Agostino MA. Ability of ultrasound in B mode and PD (PDUS) to detect erosions in mechanically strained area in healthy individuals (HI) and rheumatoid arthritis (RA): comparison with micro computed tomography scan (muCT). Ann Rheum Dis 2012;71 Suppl 3:712.
32. Finzel S, Aergeter P, Schett G, D'Agostino MA. Evaluation of physiological and abnormal cortical breaks in healthy individuals (HI) and rheumatoid arthritis (RA) patients by ultrasound in B-and PD-mode (PDUS) in comparison with micro computed tomography scan (muCT). Ann Rheum Dis 2012;71 Suppl 3:712.
33. Finzel S, Rech J, Schmidt S, Engelke K, Englbrecht M, Schett G. Interleukin-6 receptor blockade induces limited repair of bone erosions in rheumatoid arthritis: a micro CT study. Ann Rheum Dis 2013;72:396-400.
34. Finzel S, Kraus S, Schmidt S, Hueber A, Rech J, Engelke K, et al. Bone anabolic changes progress in psoriatic arthritis patients despite treatment with methotrexate or tumour necrosis factor inhibitors. Ann Rheum Dis 2013;72:1176-81.
35. Srikhum W, Virayavanich W, Burghardt AJ, Yu A, Link TM, Imboden JB, et al. Quantitative and semiquantitative bone erosion assessment on high-resolution peripheral quantitative computed tomography in rheumatoid arthritis. J Rheumatol 2013;40:408-16.
36. Toepfer D, Finzel S, Museyko O, Schett G, Engelke K. A novel technique to quantify bone erosions in patients with rheumatoid diseases using high-resolution PQCT images. Ann Rheum Dis 2012;71 Suppl 3:296.
37. Toepfer D, Finzel S, Museyko O, Schett G, Engelke K. Longitudinal quantification of bone erosions in patients with rheumatoid arthritis using high-resolution computed tomography. Arthritis Rheum 2013;65:S837.
38. Williams J, Van Rietbergen B, Arts C, Van Den Bergh J, Van Tubergen A, Scharmga A, et al. Assessment of cortical discontinuities in interphalangeal joints with HRpQCT in comparison with radiography and microct imaging [abstract]. Ann Rheum Dis 2013;72 Suppl 3:1017.
39. Zhu Y, Griffith JF, Qin L, Hung VW, Fong TN, Au SK, et al. Periarticular bone loss in female patients with rheumatoid arthritis: a case-control study using HR-pQCT [abstract]. Ann Rheum Dis 2013;72 Suppl 3:611.
40. Toepfer D, Finzel S, Museyko O, Engelke K, Schett GA. Segmentation and quantification of bone erosions in the hands of patients with rheumatoid arthritis using high resolution computed tomography [abstract]. Arthritis Rheum 2012;64 Suppl 10:S436.
41. Finzel S, Aegerter P, Schett G, D'Agostino MA. Can ultrasound (PDUS) easily detect erosions? Evaluation of physiological and abnormal cortical breaks of small joints in healthy individuals (HI) and rheumatoid arthritis (RA) patients by PDUS comparison with micro computed tomography (CT) scan [abstract]. Arthritis Rheum 2011;63 Suppl 10:S318.
42. Finzel S, Englbrecht M, Engelke K, Stach C, Schett G. A comparative study of periarticular bone lesions in rheumatoid arthritis and psoriatic arthritis. Ann Rheum Dis 2011;70:122-7.
43. Finzel S, Ernet C, Rech Sr J, Stach CM, Engelke K, Englbrecht M, et al. Comparative analysis of bone erosions and cysts in rheumatoid arthritis, psoriatic arthritis and erosive hand osteoarthritis [abstract]. Arthritis Rheum 2011;63 Suppl 10:S629.
44. Finzel S, Ohrndorf S, Englbrecht M, Stach C, Messerschmidt J, Schett G, et al. A detailed comparative study of high-resolution ultrasound and micro-computed tomography for detection of arthritic bone erosions. Arthritis Rheum 2011;63:1231-6.
45. Finzel S, Rech J, Schmidt S, Engelke K, Englbrecht M, Stach C, et al. Repair of bone erosions in rheumatoid arthritis treated with tumour necrosis factor inhibitors is based on bone apposition at the base of the erosion. Ann Rheum Dis 2011;70:1587-93.
46. Fouque-Aubert A, Boutroy S, Marotte H, Vilayphiou N, Bacchetta J, Miossec P, et al. Assessment of hand bone loss in rheumatoid arthritis by high-resolution peripheral quantitative CT. Ann Rheum Dis 2010;69:1671-6.
47. Kolling C, Stok KS, Mueller TL, Müller R, Goldhahn J. In vivo microstructural quantification of finger joints using high-resolution PQCT. J Bone Miner Res 2010;25:S141-2.
48. Stach CM, Bauerle M, Englbrecht M, Kronke G, Engelke K, Manger B, et al. Periarticular bone structure in rheumatoid arthritis patients and healthy individuals assessed by high-resolution computed tomography. Arthritis Rheum 2010;62:330-9.
49. Stach CM, Schett G. High-resolution imaging of bone erosions in rheumatoid arthritis using 3D computerized microtomography. Ann Rheum Dis 2009;68 Suppl 3:332.

APPENDIX 2.

Search Terms

a) Medline

1. Tomography, X-Ray Computed/
2. (high resolution peripheral quantitative computed tomograph* or HR PQCT or HRPQCT or Micro CT or High-Resolution Computed Tomograph* or Xtreme CT or Micro computed Tomograph*).tw.
3. 1 or 2
4. metacarpophalangeal joint/
5. wrist/
6. (metacarpophalangeal joint* or MCP* or Wrist* or Wrist Joint*).tw.
7. 4 or 5 or 6
8. 3 and 7
9. exp Escherichia coli/ or exp Chemotactic Factors/ or exp Chemokine CCL2/ or exp Metoclopramide/ or exp Cytokines/
10. 8 not 9
11. exp animals/ not humans.sh.
12. 10 not 11
13. limit 12 to English language

b) Embase

1. exp high resolution computer tomography/ or exp computer assisted tomography/
2. (high resolution peripheral quantitative computed tomograph* or HR PQCT or HRPQCT or Micro CT or High-Resolution Computed Tomograph* or Xtreme CT or Micro computed Tomograph*).tw.
3. 1 or 2
4. metacarpophalangeal joint/
5. wrist/
6. (metacarpophalangeal joint* or MCP* or Wrist* or Wrist Joint*).tw.
7. 4 or 5 or 6
8. 3 and 7
9. exp monocyte chemotactic protein 1/ or exp cytokine production/ or exp monocyte/ or exp metoclopramide/
10. 8 not 9
11. limit 10 to animal studies
12. limit 10 to (human and animal studies)
13. 11 not 12
14. 10 not 13

c) PubMed

1. ((((((metacarpophalangeal joint[MeSH Terms]) OR wrist joint[MeSH Terms]) OR ((metacarpophalangeal joint*[Title/Abstract] OR MCP*[Title/Abstract] OR Wrist*[Title/Abstract] OR Wrist Joint*)[Title/Abstract]))) AND ((Tomography, X-Ray Computed[MeSH Terms]) OR ((high resolution peripheral quantitative computed tomograph*[Title/Abstract] OR HR PQCT[Title/Abstract] OR HRPQCT[Title/Abstract] OR Micro CT[Title/Abstract] OR High-Resolution Computed Tomograph*[Title/Abstract] OR Xtreme CT[Title/Abstract] OR Micro computed Tomograph*)[Title/Abstract])))) AND "english"[Language]